

## Supplementary Information

$\beta$ -Cyclodextrin-crosslinked alginate gel for patient-controlled drug delivery systems: regulation of host-guest interactions with mechanical stimuli

Hironori Izawa, Kohsaku Kawakami, Masato Sumita, Yoshitaka Tateyama, Jonathan P Hill and

Katsuhiko Ariga

### Table of Contents

1. Instruments	···S2
2. Materials	···S2
3. Experiments	···S3
4. Preparation and characterization of CCAL and CGAL	···S7
5. Information for ODN	···S13
6. Inclusion ability of $\alpha$ - or $\beta$ -CyD toward ODN	···S14
7. Inclusion ability of CCAL toward ODN	···S19
8. Release behavior of ODN from CCAL xerogel	···S21
9. Molecular dynamics of $\beta$ -CyD in <i>vacuo</i> and bulk water	···S21
10. Geometry optimization of $\beta$ -CyD-ODN inclusion complex	···S25
11. References	···S26

## 1. Instruments

NMR spectra were obtained using an AL300 BX spectrometer (JEOL). Mass spectra were measured using a Shimadzu-Kratos Axima CFR+ MALDI-TOF mass spectrometer with 2,5-dihydroxybenzoic acid as matrix. IR spectra were obtained using a NEXUS 670-FT-IR (Thermo Nicolet). Elemental analysis data were recorded on a Perkin Elmer 2400 II CHNS/O. UV-Vis spectra were recorded on a UV-3600 UV/Vis/NIR spectrophotometer (Shimadzu). Stress-strain curves were measured using an ELS 6000 (Shimadzu) with  $1.0 \text{ mm} \cdot \text{min}^{-1}$ .

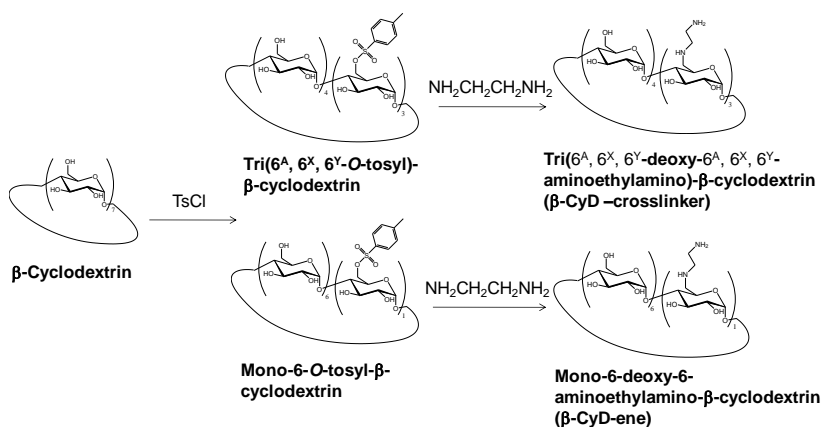
## 2. Materials

Sodium alginate (80-120 cps), 1-Ethyl-3-(3-dimethylaminopropyl)carbodiimide (EDC) ( $\geq 98\%$ ), and 2-morpholinoethanesulfonic acid (MES) ( $\geq 99\%$ ) were purchased from Wako Pure Chemical Industries (Osaka, Japan). ODN ( $\geq 98\%$ ),  $\beta$ -Cyclodextrin (CyD) ( $\geq 98\%$ ), *N*-hydroxysuccinimide (NHS) ( $\geq 98\%$ ), ethylenediamine ( $\geq 98\%$ ), and pyridine ( $\geq 99.5\%$ ) were purchased from Nacalai Tesque (Kyoto, Japan). *p*-Toluenesulfonyl chloride (TsCl) ( $\geq 99\%$ ) was purchased from Tokyo Chemical Industry Co., Ltd. (Tokyo, Japan). Other common reagents were used as received without further purification.

### 3. Experiments

#### 3-1. Synthesis of $\beta$ -CyD-crosslinker and $\beta$ -CyD-ene

$\beta$ -CyD-crosslinker and  $\beta$ -CyD-ene were prepared according to Scheme S1. Tris( $6^A$ ,  $6^X$ ,  $6^Y$ -*O*-tosyl)- $\beta$ -cyclodextrin and mono-6-*O*-tosyl- $\beta$ -cyclodextrin were prepared by conventional methods<sup>S1-S2</sup>.



**Scheme S1 | Preparation of  $\beta$ -CyD-crosslinker and  $\beta$ -CyD-ene.**

**Tris( $6^A$ ,  $6^X$ ,  $6^Y$ -deoxy- $6^A$ ,  $6^X$ ,  $6^Y$ -aminoethylamino)- $\beta$ -cyclodextrin ( $\beta$ -CyD-crosslinker).** Tris( $6^A$ ,  $6^X$ ,  $6^Y$ -*O*-tosyl)- $\beta$ -cyclodextrin (1.500 g, 0.940 mmol) was added to ethylenediamine (5.0 mL) under  $\text{N}_2$ . The mixture was stirred at  $60^\circ\text{C}$  for 12 h, and then cooled to room temperature. After cooling, the reaction mixture was poured into a large amount of ethanol to precipitate the product. The precipitate was collected by filtration, and washed with ethanol. The crude product was crystallized

from water to give product (0.671 g, 0.532 mmol) in 56.6 % yield.  $^1\text{H}$  NMR (300 MHz,  $\text{D}_2\text{O}$ , DSS)  $\delta$  = 2.57-2.66 (m, 12H,  $-\text{NHCH}_2\text{CH}_2\text{NH}_2$ ), 2.70-3.01 (m, 6H,  $-\text{CH}_2(\text{H-6}')-$ ), 3.22-3.33 (m, 3H,  $-\text{CH}(\text{H-4}')-$ ), 3.40-3.48 (m, 14H,  $-\text{CH}(\text{H-2,H-2}')-$ ,  $-\text{CH}(\text{H-5}')-$ ,  $-\text{CH}(\text{H-4})-$ ), 3.72-3.80 (m, 19H,  $-\text{CH}(\text{H-3,H-3}')-$ ,  $-\text{CH}(\text{H-5})-$ ,  $-\text{CH}_2(\text{H-6})-$ ), 4.92 (bs, 7H,  $-\text{CH}(\text{H-1, H-1}')-$ ) ppm.  $^{13}\text{C}$  NMR (75 Hz,  $\text{D}_2\text{O}$ , DSS).  $\delta$  = 36.59, 46.24, 47.10, 58.30, 68.51, 70.07, 71.37, 79.34, 81.42, 99.90 ppm. MALDI-TOF-MS (2,5-dihydroxybenzoic acid):  $m/z$ : 1261.78  $[\text{M}+\text{H}]^+$ . Elemental analysis calcd. for  $\text{C}_{48}\text{H}_{88}\text{N}_6\text{O}_{32}\cdot 6\text{H}_2\text{O}$  C 42.10 H 7.36 N 6.14, found C 42.39 H 7.62 N 5.89.

**Mono-6-deoxy-6-aminoethylamino- $\beta$ -cyclodextrin ( $\beta$ -CyD-ene).** Mono-6-*O*-tosyl- $\beta$ -cyclodextrin (1.50 g, 1.17 mmol) was added to ethylenediamine (5.00 mL) under  $\text{N}_2$ . The mixture was stirred at 60  $^\circ\text{C}$  for 12 h, and then cooled to room temperature. After cooling, the reaction mixture was poured into a large amount of ethanol to precipitate the product. The precipitate was collected by filtration, washed with ethanol and dried under reduced pressure to give product (1.21 g, 1.03 mmol) in 88.0 % yield.  $^1\text{H}$  NMR (300 MHz,  $\text{D}_2\text{O}$ , DSS)  $\delta$  = 2.61 (2H,  $-\text{NHCH}_2-$ ), 2.73 (3H,  $-\text{CH}_2\text{CH}_2\text{NH}_2$ ,  $-\text{CH}_2(\text{H-6}')-\text{N}$ ), 2.92 (d, 1H,  $-\text{CH}_2(\text{H-6}')-$ ), 3.33 (t, 1H,  $-\text{CH}(\text{H-4}')-$ ), 3.36-3.51 (m, 14H,  $-\text{CH}(\text{H-2,H-2}')-$ ,  $-\text{CH}(\text{H-5}')-$ ,  $-\text{CH}(\text{H-4})-$ ), 3.73-3.84 (m, 25H,  $-\text{CH}(\text{H-3,H-3}')-$ ,

-CH(H-5)-, -CH<sub>2</sub>(H-6)-), 4.92 (d, 7H, -CH(H-1, H-1')-) ppm. <sup>13</sup>C NMR (75 Hz, D<sub>2</sub>O, DSS). δ = 36.61, 46.22, 47.14, 58.33, 68.54, 70.09, 71.37, 79.32, 81.40, 99.89 ppm.  
MALDI-TOF-MS (2,5-dihydroxybenzoic acid): *m/z*: 1177.07 [M+H]<sup>+</sup>.

### 3-2. Preparation of CCAL and CGAL

**β-CyD-crosslinked alginate (CCAL).** In a typical reaction, AL (27.3 mg) was dissolved in 0.1 M 2-MES buffer (pH 5.6) (1.5 mL) to which EDC (20.0 mg, 104.3 μmol) and NHS (12.0 mg, 86.8 μmol) were added. After 10-minutes preactivation at room temperature, β-CyD-crosslinker (22.7 mg, 18.0 μmol) was added to the mixture with vigorous stirring. Then the reaction mixture was allowed to stand for 12 h at room temperature during which time it became a gel. The resulting hydrogel was soaked in 0.1 M aqueous Na<sub>2</sub>HPO<sub>4</sub> solution (0.1 L) at 4 °C for 1 day, followed by immersion in 1.0 M NaCl aqueous solution (0.1 L) and distilled water (1.0 L) at the same temperature. In order to confirm the structure of CCAL, the hydrogel was lyophilized to give lyophilized material (49.3 mg). <sup>1</sup>H NMR (300 MHz, NaOD-D<sub>2</sub>O, DSS, 80 °C) δ = 2.22-2.45 (6H, CyD-NCH<sub>2</sub>-), 2.50-3.11 (12H, -CH<sub>2</sub>-AL, -CH<sub>2</sub>(CyD, H-6')-), 3.12-4.90 (Sugar protons (AL, CyD), DOH), 4.91-5.13 (CyD, AL(anomeric protons)), 8.07 (-NHCO-AL) ppm. <sup>13</sup>C NMR (75 Hz, NaOD-D<sub>2</sub>O, DSS, 80 °C). δ = 36.41, 48.25, 59.27,

58.30, 64.04-82.61, 97.22-101.6, 167.21, 169.80, 174.27, 178.93, 180.00 ppm.

Elemental analysis calcd. for  $(C_6H_7NaO_6)_{4.7}(C_6H_7O_5)_{3.0}(C_{48}H_{85}N_6O_{32})_{1.0} \cdot 15H_2O$  C

38.51 H 5.81 N 2.86, found C 38.41 H 6.20 N 3.07.

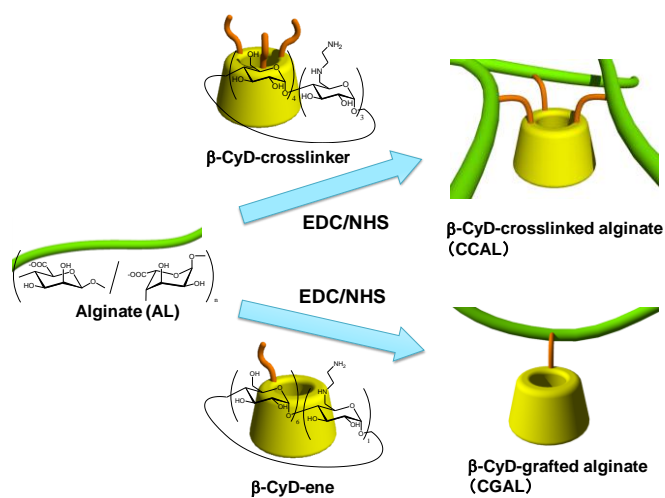
**$\beta$ -CyD-grafted alginate (CGAL).** Typically, AL (27.3 mg) was dissolved in 0.1 M 2-morpholinoethanesulfonic acid (MES) buffer (pH 5.6) (1.5 mL) to which EDC (20.0 mg, 104.3  $\mu$ mol) and NHS (12.0 mg, 86.8  $\mu$ mol) were added. After 10-minutes preactivation at room temperature,  $\beta$ -CyD-ene (22.7 mg, 19.3  $\mu$ mol) was added to the mixture with vigorous stirring. Then the reaction mixture was allowed to stand for 1 day at room temperature until a gel state was achieved due to ionic interactions. The resulting hydrogel was soaked in 0.1 M aqueous  $Na_2HPO_4$  solution (0.1 L) at 4 °C for 1 day, followed by immersion in 1.0 M NaCl aqueous solution (0.1 L). In order to confirm the structure of CGAL, the hydrogel was desalted by dialysis, and lyophilized to give lyophilized material (42.3 mg).  $^1H$  NMR (300 MHz, NaOD- $D_2O$ , DSS, 80 °C)  $\delta$  = 2.21-2.43 (2H, CyD- $NCH_2^-$ ), 2.50-3.10 (4H,  $-CH_2-AL$ ,  $-CH_2(CyD, H-6')^-$ ), 3.12-4.91 (Sugar protons (AL, CyD), DOH), 4.92-5.10 (CyD, AL(anomeric protons)) ppm.  $^{13}C$  NMR (75 Hz, NaOD- $D_2O$ , DSS, 80 °C).  $\delta$  = 36.42, 48.27, 59.27, 58.31, 64.04-82.61, 97.21-101.5, 167.21, 169.81, 174.23, 178.91, 180.02 ppm.

#### 4. Preparation and characterization of CCAL and CGAL

Various CCALs with different feed AL/ $\beta$ -CyD-crosslinker ratios were prepared by dehydrating condensation reaction between alginate (AL) and  $\beta$ -CyD-crosslinker with 1-ethyl-3-(3-dimethylaminopropyl)carbodiimide (EDC) and *N*-hydroxysuccinimide (NHS) (Scheme S2, Table S1). Consequently, viscous solutions became gelatinous (Figure S1). After removing impurities originating from the condensation reaction (such as EDC and NHS), unreacted-carboxyl groups in the CCALs were estimated by a titration method<sup>3</sup>. In all cases, estimated values of unreacted carboxyl groups showed good agreement with differences of carboxyl groups in AL and ethylenediamino groups in  $\beta$ -CyD-crosslinker, suggesting that almost all terminal amino groups had reacted with carboxyl groups in CCALs. In order to further confirm the production of CCAL, the CCALs obtained were lyophilized. The weights of lyophilized materials were also in good agreement with feed amounts of AL and  $\beta$ -CyD-crosslinker. Furthermore, production of CCAL was confirmed by NMR (Figure S3, Figure S4), IR (Figure S5), and elemental analysis (shown in section 3) of the lyophilized material. Figure S6 shows the stress-strain curves of hydrogels obtained under compressive mode. In the compressive tests, larger Young's moduli and fracture stress values were recorded with an increasing amount of  $\beta$ -CyD-crosslinker, indicating that the crosslinking reaction

enhances the gels' strength although they were still too weak to resist repeated compressions. Hydrogels were strengthened by complexation with  $\text{Ca}^{2+}$  by soaking in 10 mM aqueous  $\text{CaCl}_2$  solution (Figure S2a). Moduli of CCALs after conversion complexation with  $\text{Ca}^{2+}$  were much higher (2.0-2.6 kPa) than those for the  $\text{Na}^+$  form (0.1-0.5 kPa). We assume that the presence of intra-crosslinking points through covalent bonds offers greater dynamicity at the junction points and/or flexibility of  $\beta$ -CyD-crosslinker contributes to the softness of the covalently  $\text{Na}^+$ -crosslinked gel. CCAL xerogel was prepared by lyophilization (Figure S2b). CCAL xerogel does not readily return to its original hydrogel state upon contact with water probably due to the strength of its hydrogen-bond network, and is a sponge-like material (Fig. S2c). In addition, various CGALs with different feed AL/ $\beta$ -CyD-ene ratios were prepared in the same manner (Table S2).





**Scheme S2 | Preparation of CCAL and CGAL.**

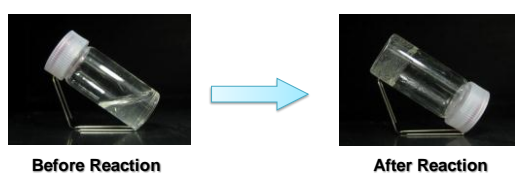


**Figure S1 | Hydrogelation of AL aqueous solution by crosslinking reaction with  $\beta$ -CyD-crosslinker.**

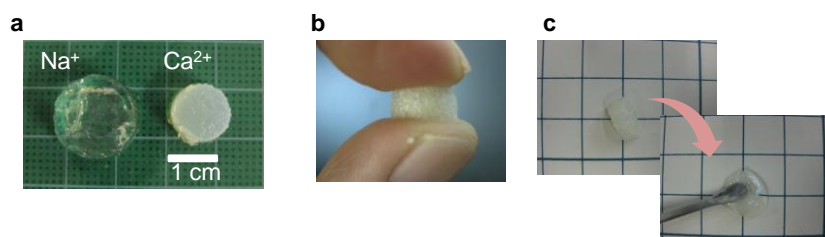


**Figure S2 | Images of CCALs. Na<sup>+</sup>(left) and Ca<sup>2+</sup> form of CCALs. Scale bar = 1 cm.**

**Table S1 | Preparation and characterizations of CCALs.**

Sample	AL β-CyD-crosslinker (mg : mg)	/ Carboxyl group / Ethylenediamino group (mol/mol)	Unreacted carboxyl group* (%)	Water content		Young's modulus	
				(%)		(kPa)	
				Na <sup>+</sup> form	Ca <sup>2+</sup> form	Na <sup>+</sup> form	Ca <sup>2+</sup> form
1	38.7 : 11.3	7.2	85.5	97.5	93.7	0.1	2.6
2	33.0 : 17.0	4.2	75.2	97.3	92.8	0.4	2.4
3	27.3 : 22.7	2.6	63.0	96.8	92.1	0.5	2.0
4 <sup>†</sup>	21.6 : 28.4	1.6	ND	-	-	-	-

\* Estimated by titration method.<sup>S3</sup> † Not gelled. Products were precipitated out from reaction solution.

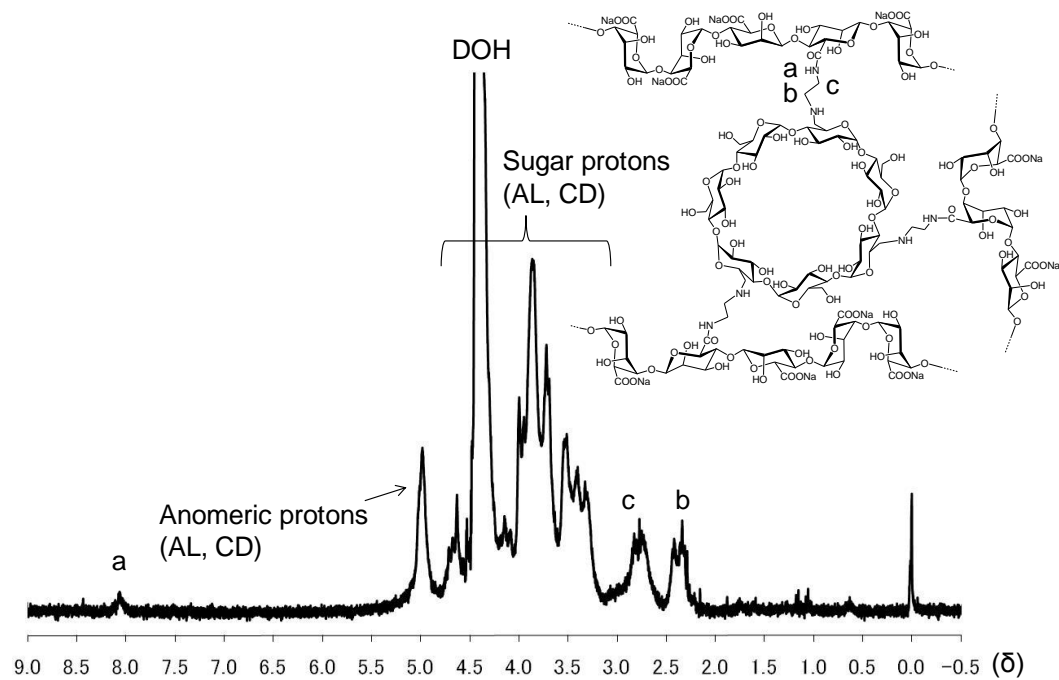


**Figure S3 | <sup>1</sup>H NMR spectrum of CCAL in 10 mM NaOD/D<sub>2</sub>O at 80 °C.**

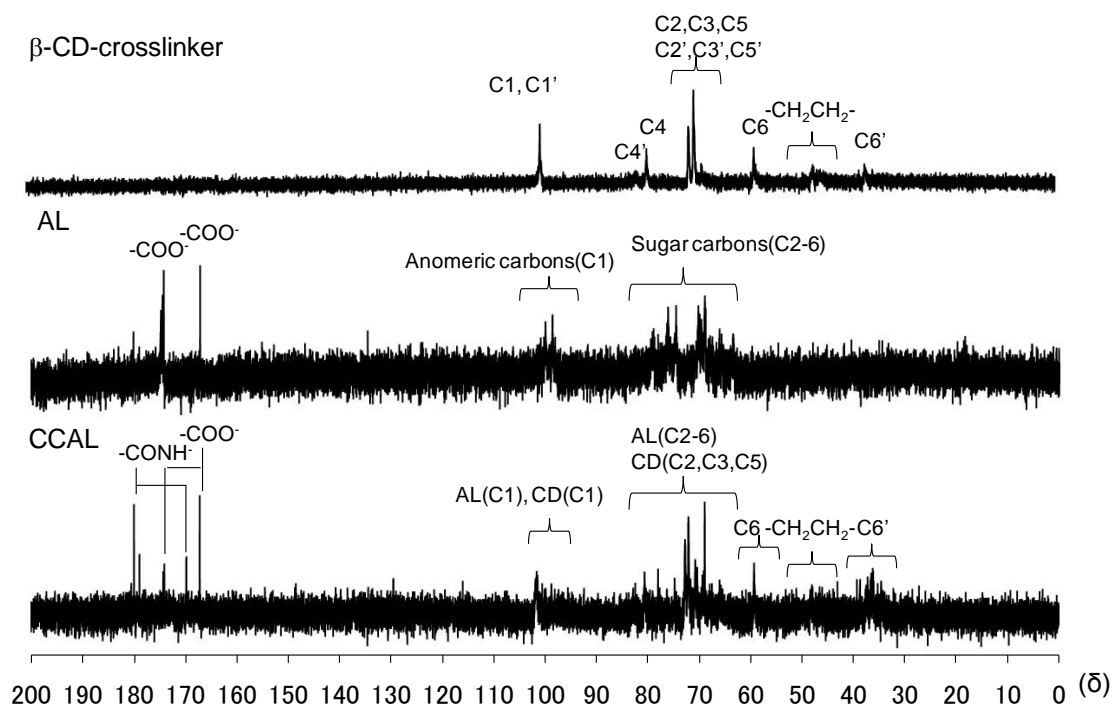


**Figure S4** |  $^{13}\text{C}$  NMR spectra of  $\beta\text{-CyD}$ -crosslinker, AL, and CCAL.

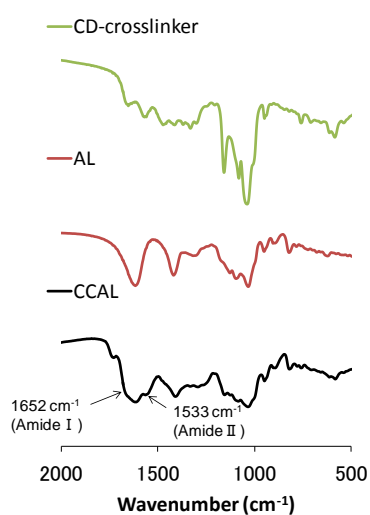


**Figure S5** | IR spectra of  $\beta\text{-CyD}$ -crosslinker, AL, and CCAL.

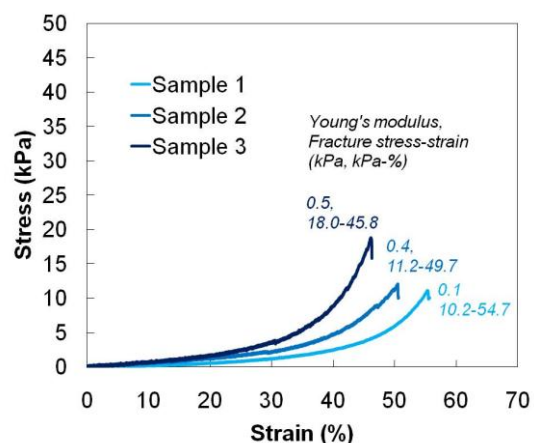


**Figure S6** | Stress-strain curves of Na<sup>+</sup> form of CCALs under compressive mode at 37 °C. AL/ $\beta$ -CyD-crosslinker ratios in weights were 3.4 (Sample 1), 1.9 (Sample 2), and 1.2 (Sample 3).

**Table S2** | Preparation and characterizations of CGALs.

Sample	AL / $\beta$ -CyD-ene (mg : mg)	Carboxyl group / Ethylenediamino group (mol/mol)	Unreacted carboxyl group* (%)	Water content (%)		Young's modulus (kPa)	
				Na <sup>+</sup> form	Ca <sup>2+</sup> form	Na <sup>+</sup> form	Ca <sup>2+</sup> form
1'	38.7 : 11.3	20.3	95.8	98.3	96.2	ND	3.4
2'	33.0 : 17.0	11.5	92.4	98.1	96.1	ND	3.0
3'	27.3 : 22.7	7.1	86.5	97.8	95.9	ND	2.8

\* Estimated by titration method.<sup>S3</sup>

## 5. Information for ODN

Excess quantities of ODN were added to various aqueous buffer solutions (pH 5.0-7.0), and the solutions were stirred at 37 °C for 1 week. The solutions were centrifuged, and the supernatants were assayed by UV-Vis measurement after appropriate dilution (Figure S7a). The solubility of ODN was strongly dependent on pH in the pH range of 5.0-7.0. On the other hand, Figure 7b shows a standard curve for ODN at 312 nm in phosphate buffer (pH 6.5). Estimated molar absorptivity was ca 13,000  $\text{M}^{-1} \text{cm}^{-1}$ .

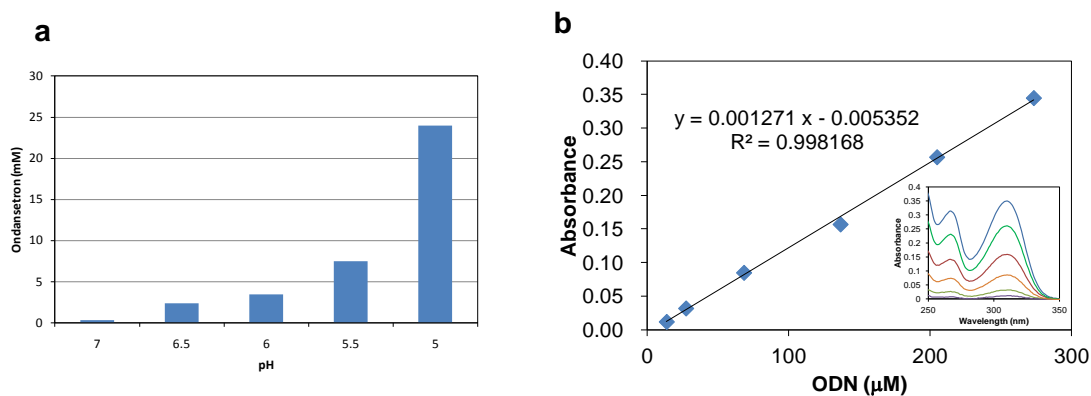


**Figure S7 | Solubility of ODN in various pH of aqueous buffer solutions at 37 °C (a) and standard curve of ODN in phosphate buffer (pH 6.5) in a cell with 1 mm optical length (b).**

## 6. Inclusion ability of $\alpha$ - or $\beta$ -CyD toward ODN

The stoichiometry and binding constants  $K$  ( $M^{-1}$ ) between  $\alpha$ - or  $\beta$ -CyD and ODN in phosphate buffer solution (pH 6.5) at 37 °C were estimated from phase solubility study<sup>S4</sup> (Figure S8) and absorbance<sup>S5</sup> (Figure S9). In the former procedure, binding constant for the 1:1 complex was calculated from the slope using the following equation, where  $S_0$  is the intrinsic solubility of the drug.

$$K_{ab} = \frac{\text{slope}}{S_0(1 - \text{slope})}$$

In the later procedure, binding constant could be evaluated from a Benesi-Hildebrand type equation:

$$\frac{[Guest] \cdot L}{A - A_0} = \frac{1}{K \cdot \varepsilon \cdot [CD]} + \frac{1}{\varepsilon}$$

where  $A$ ,  $A_0$ , and  $\varepsilon$  are the absorbance of guest in the presence and absence of  $\beta$ -CyD, and molecular extinction coefficient, respectively. Good linearities of plots were observed for both methods, suggesting the formation of inclusion complex with a 1:1 stoichiometry. In addition, binding constants estimated from both methods showed similar values (Table S3). Binding constants between  $\alpha$ -CyD and ODN were much smaller than those for  $\beta$ -CyD. These results clearly indicate that  $\beta$ -CyD is more suitable than  $\alpha$ -CyD for formation of an inclusion complex with ODN most likely due to their differing cavity sizes.

In order to obtain further information on complex formation,  $^1\text{H}$  NMR analyses were performed (Figure S10, S11). In the  $^1\text{H}$  NMR spectrum of the solution containing 2.0 mM ODN and 0.4 mM  $\beta$ -CyD, signals due to inner protons (H-3, H-5) were shifted to higher field (Figure S10a), clearly indicating that  $\beta$ -CyD formed an inclusion complex with ODN.<sup>S6</sup> Furthermore, in the spectrum of the solution containing 2.0 mM ODN and 10.0 mM  $\beta$ -CyD, the signals attributed to carbazole protons (a, e, f, g) were notably shifted to lower field (Figure S11, Table 4). These results and the geometry optimization of  $\beta$ -CyD-ODN inclusion complex (*vide infra*) provide the predicted structures of inclusion complexes as shown in Figure S12.

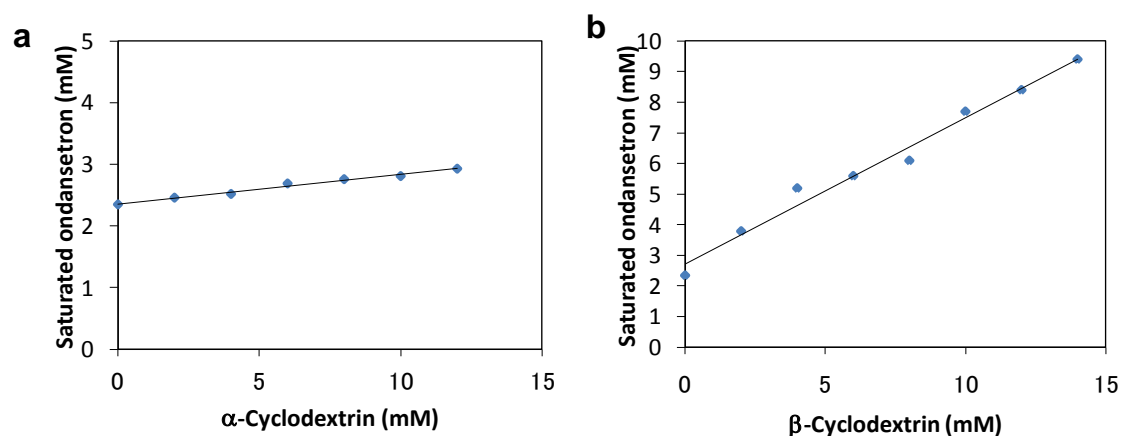


**Figure S8** | Phase solubility diagrams of ODN as a function of  $\alpha$ -CyD (a) or  $\beta$ -CyD

(b).

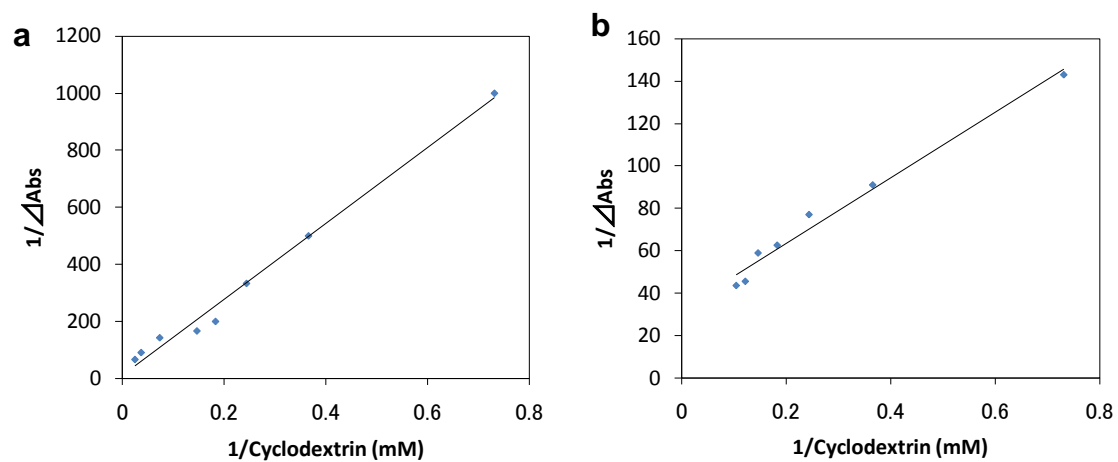


**Figure S9** | Benesi-Hildebrand type plots for ODN in phosphate buffer solution (pH 6.5) containing various concentration of  $\alpha$ -CyD (a) or  $\beta$ -CyD (b) at 37 °C.

**Table S3** | Estimated binding constants between  $\alpha$ - or  $\beta$ -CyD and ODN.

Phase	Binding constant ( $\text{M}^{-1}$ )	
	solubility	Absorbance change <sup>S5</sup>
$\alpha$ -CyD	18.6	10,1
$\beta$ -CyD	339.0	212.4





**Table S4** | Chemical shifts of  $\beta$ -CyD-ODN complex in  $^1\text{H}$  NMR spectra.

	Chemical shift (ppm)		$\Delta\delta$ (ppm)
	ODN (2.0 mM)	ODN : $\beta$ -CyD (2.0 mM: 10.0 mM)	
g	2.181	2.236	0.055
j	2.493	2.512	0.019
f	2.836	2.911	0.075
e	3.524	3.643	0.119
k	4.218	4.230	0.012
h	7.382	7.405	0.023
a	7.854	7.981	0.127

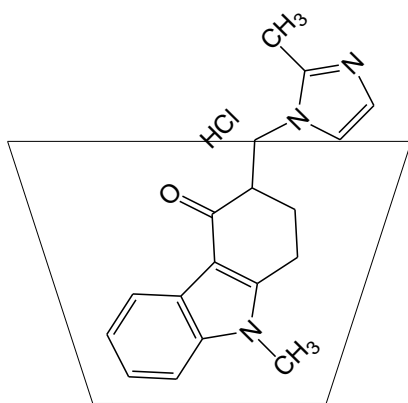


**Figure S12** | Predicted major complex of ODN and  $\beta$ -CyD.

## 7. Inclusion ability of CCAL toward ODN

The inclusion ability of  $\beta$ -CyD moieties in the CCAL was confirmed by UV-Vis and  $^1\text{H}$  NMR spectra (Figure S13, S14). As described above,  $\beta$ -CyD forms a 1:1 complex with ODN in aqueous solution and induces a blue shift of absorptions of ODN in its UV-Vis spectrum. Blue shifts also occur in the case of CCALs, suggesting that the  $\beta$ -CyD moieties in CCAL form inclusion complexes with ODN. Although  $^1\text{H}$  NMR signals of ODN with CCAL (Sample 3) used for release experiments could not be observed in  $\text{D}_2\text{O}$  phosphate buffer solution (pD 6.5) at 37 °C because of the low resolution of the hydrogel state in the NMR measurement, we could observe them in CCAL having fewer junction points ( $\text{AL}/\beta\text{-CyD-crosslinker} = 10$ ) (Figure S14). In the spectrum, shifts in the signals attributed to benzene ring proton (a; large shift) and methyl protons of imidazolium (j; small shift) were observed, which was similar to the case for the spectrum of a mixture of ODN and  $\beta$ -CyD. This result suggests that the structure of the inclusion complex of the  $\beta$ -CD-moieties in CCAL with ODN is almost the same as that in the mixture of  $\beta$ -CyD and ODN as shown in Figure S12.

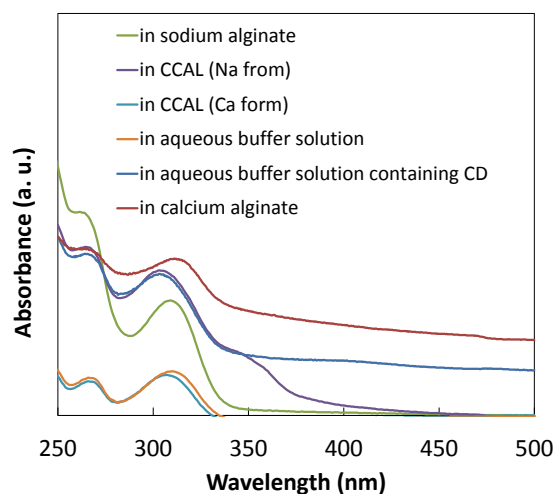


**Figure S13** | UV-Vis spectra of ODN in various solutions or hydrogels. UV-Vis spectra were obtained using a Quartz cell (1 mm pathlength) for solutions, while the hydrogels were sliced (ca. 1 mm thickness) for the measurements. 75.0  $\mu\text{M}$  or 200.0  $\mu\text{M}$  ODN solutions (pH 6.5) containing 300.0  $\mu\text{M}$   $\beta$ -CyD or 92.0  $\mu\text{M}$  sodium alginate, respectively, were used for the measurement. The AL and CCALs were soaked in 320.0  $\mu\text{M}$  ODN solutions (pH 6.5) to load ODN.

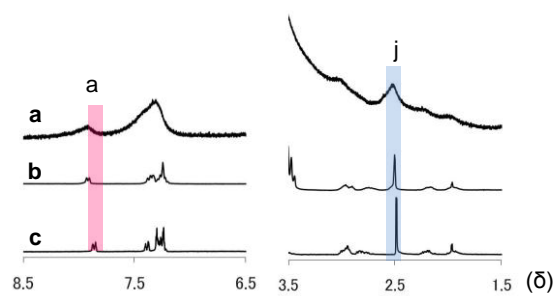


**Figure S14** |  $^1\text{H}$  NMR spectra of the mixture of 2.0 mM ODN and 2.0 mM CCAL (as concentration of  $\beta$ -CyD moieties) (a), the mixture of 2.0 mM ODN and 2.0 mM  $\beta$ -CyD (b), and ODN (c) in  $\text{D}_2\text{O}$  phosphate buffer solution (pD 6.5) at 37  $^\circ\text{C}$ .

## 8. Release behaviour of ODN from CCAL xerogel

CCAL xerogel (Sample 3) as shown in Figure S2b-c was soaked in 5.5 mM ODN aqueous solution (10 mM phosphate buffer) (1 mL) at 4 °C for 2 days to load ODN. The ODN-loaded xerogel was subjected to release study in phosphate buffer solution (pH 6.5) (50 mL) at 37 °C for 2 days. The xerogel was pressed after 25 h, 27 h, 29 h for 5 min to observe release. Release rate was not changed by mechanical stimuli.

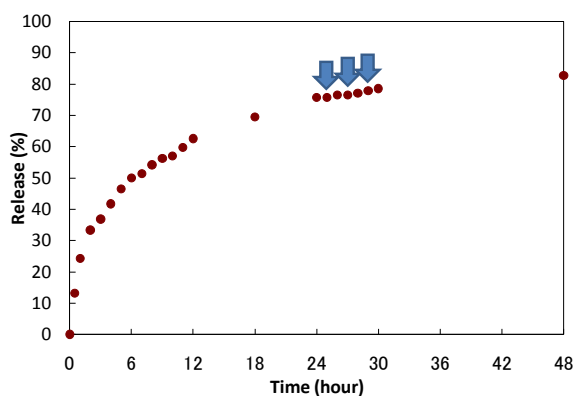


**Figure S15** | Release of ODN from xerogel of CCAL by mechanical stimuli.

## 9. Molecular dynamics of $\beta$ -CyD in *vacuo* and bulk water

To investigate the flexibility of  $\beta$ -CyD in *vacuo* and bulk water, we performed first-principles molecular dynamics simulations using density functional theory (DFT) methods implemented in CPMD.<sup>S7</sup> Total energies were calculated at the  $\Gamma$  point in a super cell approach by using BLYP generalized gradient corrected exchange-correlation functional. The Kohn-Sham orbitals were expanded by plane wave basis set up to the

energy cutoff of 70 Ry. Troullier-Martin type norm-conserving pseudopotentials were used for all atoms.

For dynamics, we used the Nosé-Hoover thermostat<sup>S8</sup> at a temperature of 309 K for NVT ensemble. The time step was set at 5 a.u. The fictitious mass of electrons in Car-Parrinello dynamics<sup>S9</sup> was 500 a.u. After equilibration for a few picoseconds (ca. 3 ps), we obtained the equilibrium trajectories, which were used to carry out sampling.

We used a cubic cell with dimensions of 30×30×30 Å for these systems. H<sub>2</sub>O molecules are added after obtaining the equilibrium condition *in vacuo* so that the density of H<sub>2</sub>O reaches an ambient condition.

All internal hydrogen bonds between OH (2-position)---OH (3'-position) were present in the calculated structure of β-CyD *in vacuo*, whereas one was broken in bulk water because of hydrogen bonding with a water molecule (see Figure S16). Furthermore, hydrogen bonding between water molecules and OH groups at 6-positions are shown. We suppose that these hydrogen bonds with water molecules result in flexibility of the β-CyD structure to strain caused by an external stress in CCAL. Calculated distributions of inner perimeters estimated by connecting inner protons at 3-positions or 5-positions of glucose units in β-CyD in bulk water were different from those *in vacuo* where the inner perimeter, based on 3-positions in bulk water, became

shorter probably due to interaction between  $\beta$ -CyD and water molecules, and remaining internal hydrogen bonds between OH (2-position)---OH (3'-position) (Figure S17). On the other hand, there is not a large difference between the distributions of 5-positions *in vacuo* and in bulk water. That is, the structure of  $\beta$ -CyD in bulk water is more cylindrical than *in vacuo*. Thus, we suppose that the mobility of  $\beta$ -CyD in bulk water is very high because of hydration.

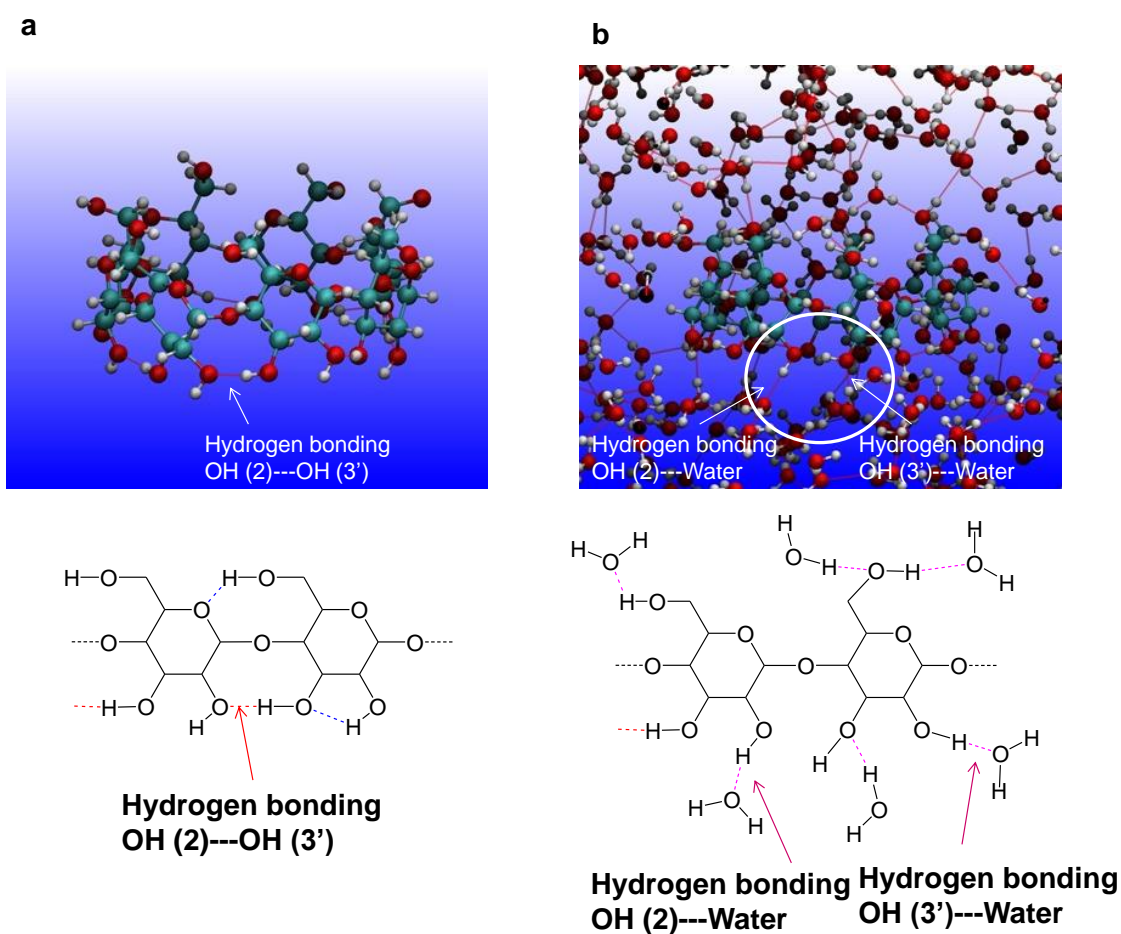


**Figure S16** | Calculated structure of  $\beta$ -CyD in *vacuo* (a) and in bulk water (b).

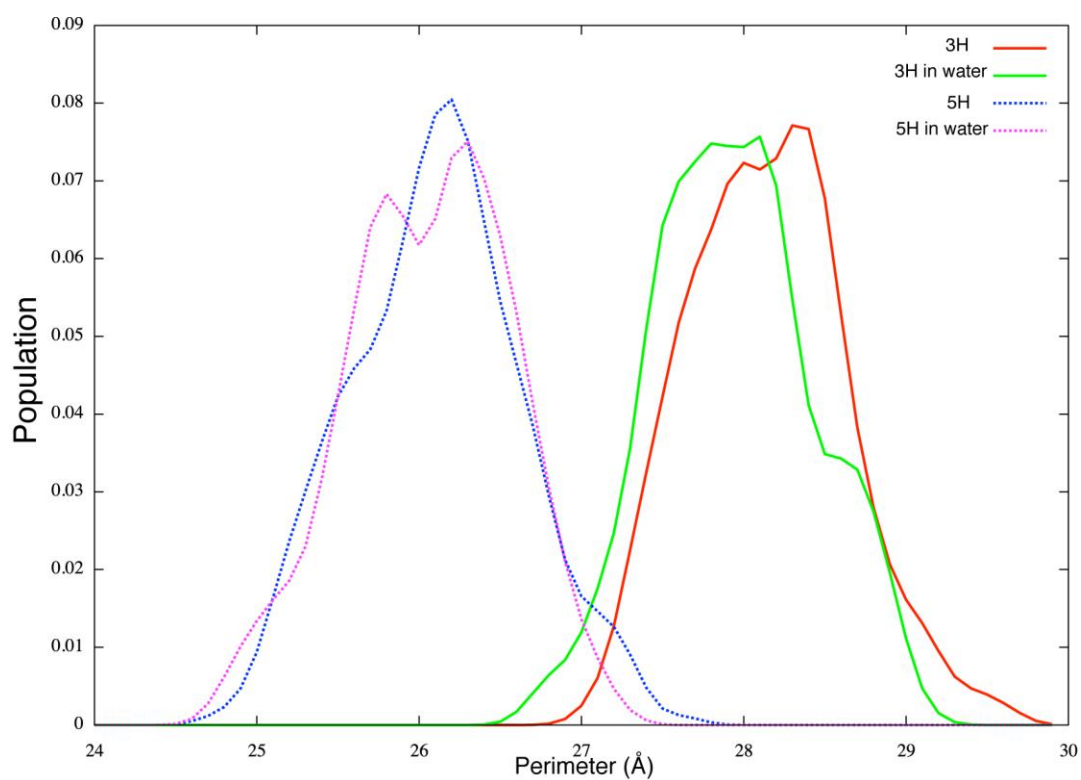


**Figure S17** | Calculated distributions of inner perimeters estimated by connecting all 3Hs or 5Hs of glucose units in  $\beta$ -CyD in *vacuo* and in bulk water.



## 10. Geometry optimization of $\beta$ -CyD-ODN inclusion complex

Geometry optimization of  $\beta$ -CyD-ODN inclusion complex *in vacuo* was carried out at the DFT/BLYP/6-31G\* level<sup>S10</sup> to provide the same structure as that expected from <sup>1</sup>H NMR measurement.

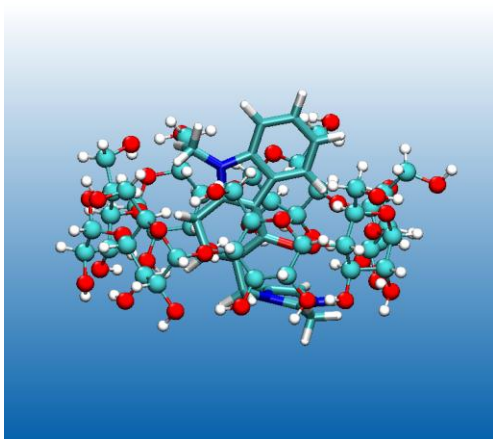


**Figure S18** | Calculated structure of the  $\beta$ -CyD-ODN inclusion complex *in vacuo*.

## 11. References

- S1 Fujita, K., Tahara, T. & Koga, T. Regioisomeric 6a,6x,6y-Tri-O-Sulfonylated Beta-Cyclodextrin. *Chem Lett*, 821-824 (1989).
- S2 Matsui, Y., Yokoi, T. & Mochida, K. Catalytic Properties of a Cu(Ii) Complex with a Modified Cyclodextrin. *Chem Lett*, 1037-1040 (1976).
- S3 Saito, T., Kimura, S., Nishiyama, Y. & Isogai, A. Cellulose nanofibers prepared by TEMPO-mediated oxidation of native cellulose. *Biomacromolecules* **8**, 2485-2491, doi:Doi 10.1021/Bm0703970 (2007).
- S4 Higuchi, T. & Kristian.H. Binding Specificity between Small Organic Solutes in Aqueous Solution - Classification of Some Solutes into 2 Groups According to Binding Tendencies. *J Pharm Sci* **59**, 1601-& (1970).
- S5 Benesi, H. A. & Hildebrand, J. H. A Spectrophotometric Investigation of the Interaction of Iodine with Aromatic Hydrocarbons. *J Am Chem Soc* **71**, 2703-2707 (1949).
- S6 Salvatierra, D., Jaime, C., Virgili, A. & SanchezFerrando, F. Determination of the inclusion geometry for the beta-cyclodextrin benzoic acid complex by NMR and molecular modeling. *J Org Chem* **61**, 9578-9581 (1996).
- S7 CPMD V3.15.1: IBM Research division, MPI Festkoerperforschung Stuttgart: <http://www.cpmc.org>
- S8 Louie, S. G., Froyen, S., Cohen, M. L. *Phys. Rev. B*, **26**, 1738 (1982)
- S9 Car. R.; Parrinello, M. *Phys. Rev. Lett.* **55**, 2471 (1985)
- S10 Frish, M. J. et al. GAUSSIAN 09, Revision A02, Gaussian, Inc., Wallingford, CT, 2004.